

Rate Studies of the Decomposition of Ammonia and Methane in a Plasma Jet

M. P. FREEMAN and J. F. SKRIVAN

American Cyanamid Company, Stamford, Connecticut

It quickly becomes apparent to the investigator of plasma jet chemistry that the head or arc device is an extremely harsh chemical environment and is otherwise not well suited to the investigation of subtle nuances. This fact suggests the introduction of reagents into the plasma downstream of the head in the intermediate section for exploratory work. The investigator becomes embroiled in apparently contradictory and confusing results however, because two intermediate sections fed with the same plasma and reagent streams at the same power levels may give entirely different product distributions.

In an attempt to develop a systematic means of characterizing intermediate sections a careful investigation of their comparative efficiency in cracking ammonia was undertaken. Surprisingly the data correlated well, and kinetic interpretation of the data appeared feasible.

This paper reports such an investigation for a particular kind of intermediate section, the tube confined plasma jet with radial feed of reagent. The observed cracking behavior is first interpreted (unsuccessfully) as a first-order dissociation rate limited reaction and then as a diffusion rate controlled reaction. It is possible to evaluate all parameters in the second model, and they appear to be of reasonable magnitude, lending credulity to this model. If one accepts this model, it is possible to calculate several quantities of interest about the reactor. These are the distribution of times reagent molecules and their products spend in the reaction zone, the average residence times, the distribution of temperatures first encountered by reagent molecules diffusing into the zone, and finally the axial temperature profile of the effluent plasma.

The ammonia-cracking study was chosen for careful work because of the accuracy with which the ammonia content of a gas stream may be analyzed and the simple nature of the reaction, since nitrogen and hydrogen are the only products. Also reported here are methane-cracking data, but the precision is of somewhat lower order than for the ammonia study, and these data are primarily included to show the

qualitative agreement with the cracking behavior of ammonia.

EXPERIMENTAL

The plasma jet unit is powered by rectified 3 ϕ alternating current from two 12 kw. arc-welding power supplies. The arc unit is the N-4 head in which the earlier style of thoriated tungsten cathode and anode is used. The front electrode through which the plasma emerges is used as the anode. A schematic diagram of the arc chamber is shown in Figure 1. Argon (99.997% pure) enters the arc chamber tangentially at a flow rate of about 1 g. mole/min., passes through the arc and exits through the front electrode, firing directly into the intermediate section. The latter consists of three 2 in. water-cooled sections (represented as a single piece in Figure 1) connected in series and having an inside diameter of $\frac{1}{4}$ in., to conform to the front electrode orifice. The first section is equipped with a $\frac{1}{8}$ in. I.D. radial feed tube centered 1.43 cm. from the inlet to the section.

Reagent gas (anhydrous ammonia, 99.98%, or methane, 99.0%) is fed to the intermediate section through the radial feed inlet. The resultant mixture of argon, reagent, and cracking products passes from the reactor into a heat exchanger where its temperature is reduced to within a few degrees of ambient. The gas is subsequently vented through a steam jet ejector system which is also used as a pump for subatmospheric runs.

The argon flow rate is metered by an orifice gauge calibrated by water displacement to less than 1% probable error. Reagent gas flows are determined by analysis of the off gas with the arc extinguished (with argon as the reference gas) but are preset by calibrated rotameters. The static pressure in the system is determined by a mercury manometer connected to the heat exchanger. Under the operating conditions used the pressure drop through the intermediate section is found to be negligible. The runs are made at two nominal values for the total pressure, 760 and 300 mm. Hg.

The net heat flow in the plasma at any exit point of a water-cooled section of a plasma train such as is described here may be determined by a heat balance technique. Specifically (neglecting the small effect of power supply ripple) one gets

$$q = EI - 4.186 \sum_{i=0}^n F_i c \Delta T_i \quad (1)$$

where the summation extends over all water-cooled sections up to the point of interest. Thus taking the zeroth section to be the head (arc chamber) itself, and i

to be 1, 2, and 3 for the three piece intermediate section, one may determine the heat flow in watts at the exit of the head and at the exit of each of the three sections by inclusion of succeeding terms in Equation (1). A calibrated orifice gauge meters the head water supply, while calibrated rotameters meter the water supplies which are feeding the heat exchanger and the parts of the intermediate section. The temperature rise in any water-cooled section is determined with in-line thermometers. If one uses the meters provided with the equipment, the electrical power input is known within $\pm 2\%$, whereas other factors combine to give a probable uncertainty of $\pm 5\%$ in an overall heat balance as determined at the exit to the heat exchanger.

For use in kinetic studies an analytic function describing the axial heat flow profile throughout the length of the reactor is desirable. A comprehensive study of the heat transfer from a plasma to a confining water-cooled tube (as yet unpublished) yielded the empirical equation

$$z + s = s(h_0/h)^{3/2} = s(q_0/q)^{3/2} \quad (2)$$

Important though this relationship is to the present paper, a full discussion of its origin would be irrelevant. The validity of the relationship for the apparatus used here is indicated in Figure 2 however. The same plasma jet device is fired at a roughly constant power level down a series of $\frac{1}{4}$ in. I.D. water-cooled copper tubes of various length. The average excess enthalpy of the argon at the exit is determined from the known mass flow and the residual heat flow. This is plotted vs. tube length plus s logarithmically, while the line is drawn with slope and intercept predicted by Equation (2). Clearly the fit is satisfactory. The study revealed furthermore that relation (2) was independent of pressure and composition of the plasma (argon, nitrogen, and hydrogen were all used). Its use would therefore seem justified for a mixture of argon, ammonia (or methane), and cracking products.

At the temperatures involved in a plasma jet all heat capacities are approaching their theoretical maximum and hence are reasonably constant. One may obtain a useful approximate relationship by substituting temperature in degrees centigrade for excess enthalpy in Equation (2):

$$z + s = s(t_0/t)^{3/2} \quad (3)$$

Degree of conversion

An important datum is y . This is obtained from the ammonia runs by first analyzing the off gas for its ammonia con-

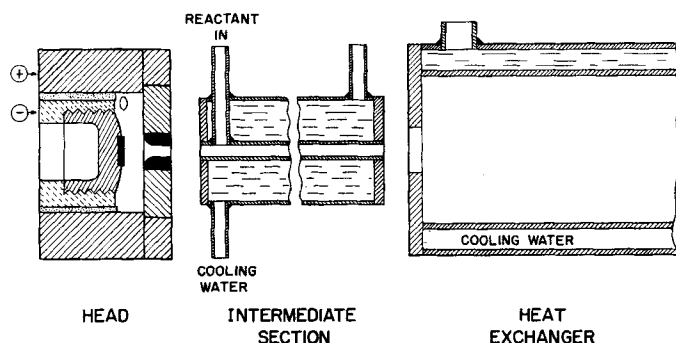


Fig. 1. Schematic representation of a tube confined plasma jet.

tent and then, together with the known stoichiometry of the reaction and the known initial composition, computing y . That the stoichiometry is given by two moles of ammonia going to one of nitrogen and three of hydrogen with no appreciable formation of other products has been verified by mass spectrometry. For the analysis a mercury displacement pump was used to withdraw a 522 ml. gaseous aliquot at the total pressure of the heat exchanger from a sample tap located in its side. This sample was then analyzed for ammonia partial pressure by standard wet analysis techniques. For checking purposes the system was filled with ammonia, and it was determined that the method is accurate to within 1% at the two pressures used in this experiment. Analyses taken in the case of the system filled with ammonia and flushed with dilute mixtures of ammonia in argon at typical flow rates show that the final composition is reached within 8 min. For all ammonia runs reported here 12 min. were allowed to lapse between changing reagent partial pressure and/or power level and sampling.

In the case of the methane decomposition the overall stoichiometry is not as well defined because the product distribution is a function of power input. However the presence of argon as an internal standard simplified the problem of determining methane conversions. With the laboratory gas chromatographic facility, the partial pressure of methane relative to that of argon is determined. For a run this pressure ratio divided by that obtained with the same flow rates and the arc extinguished was just the desired fraction y . Analytical samples for the chromatograph were taken by a peristaltic pump from the sample tap in the heat exchanger. The analyses were checked for internal consistency by doing a total carbon balance among the products of the decomposition. Nearly half the runs were discarded for deviating more than 10% from a material balance presumably because of analytical limitations. In the kinetic analyses only those points coming within 5% of a material balance were actually used in correlating the data, although the order points are shown on the plot as filled circles.

RESULTS

The data for the cracking of ammonia at 760 mm. Hg total pressure and of ammonia and methane at 300 mm. Hg total pressure are tabulated in

the appendix.* Given are values of n_{A0} , n_{G0} , q_0 , and y .

Dissociation Kinetics Model

Theory. The observation of mixing behavior in a transparent tubular reactor, for example, prompts the notion that mixing is very rapid, and so it seemed natural at first to assume that the decompositions of the reagent gases were rate limited by normal dissociation kinetics.

The model for this case assumes immediate mixing between reagent and argon plasma. A mixed mean temperature at the point of mixing is computed from the known flow rates of the gases, the heat flow at the feed point, and tables of enthalpy (h) vs. temperature for the gases involved. It is assumed that the decomposition is homogeneous, first order and that each molecule reacting goes immediately to its final stoichiometry. Because of the large sensible heats involved and the relatively low concentration of reagent gas the heat of reaction is neglected, an assumption somewhat better for ammonia than for methane.

A flow reactor poses special problems for the kineticist, but these have

* Tabular material has been deposited as document 7214 with the American Documentation Institute, Photoduplication Service, Library of Congress, Washington 25, D. C., and may be obtained for \$1.25 for photoprints or for 35-mm. microfilm.

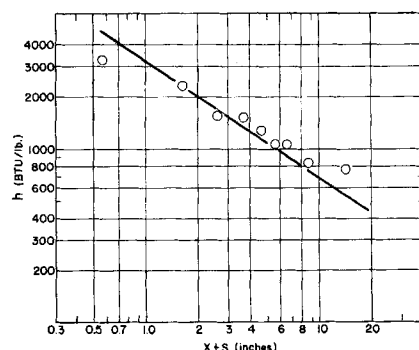


Fig. 2. A logarithmic plot of excess enthalpy at the exit vs. $z + s$ for an argon jet in $\frac{1}{4}$ in. I.D. intermediate sections of various lengths z at constant input enthalpy h_0 . This plot comes from the heat transfer study alluded to in the text. Note the use of different units.

been solved for an isothermal flow reactor (2) and can be equally well solved for a nonisothermal reactor if an expression for the rate constant valid over a range of temperatures is employed (3). The (mixed mean) temperature profile in the reactor is approximated from Equation (3), while the integration of the rate expression is performed from an adjustable point of mixing and extends to infinity. Suitable processing of the data then reveals something about the magnitude of the decomposition probability of an excited molecule (3) (equivalent to the pre-exponential factor in the Arrhenius rate expression) and the activation energy.

Results. The activation energies determined by the method above are on the order of 9 kcal. for both ammonia and methane, about 0.1 of a reasonable value for either. Furthermore the calculated rate of reaction is much higher than that observed. This is in contradiction to the results obtained by Holsen et al. (4) for the decomposition of ammonia in a chemical shock tube in an overlapping temperature range, for if the number of effective oscillators is given the value of 2, their data conform exactly to the rate expression given in reference 3 for an activation energy of 80 kcal/mole, an altogether reasonable value. Similarly predictable results have been obtained by other authors working with methane (5), so it must be concluded that the model is wrong.

Naturally a number of modifications of the model were tried in an attempt to see where the discrepancy arises. They were either ineffective in raising the calculated activation energy, or else they caused a direct departure from model. One pertinent fact learned from these attempts however is that the mixed mean temperature as calculated above seems to be significant. An attempt at altering the effective heat capacity of the ammonia results in increasing the scatter of the data points.

Diffusional Model

Theory. When both the activation energy and the reaction rate are substantially lower than anticipated, it is appropriate to investigate possible diffusional mechanisms as rate-limiting steps, for it is of course impossible to observe a rate of reaction greater than the rate of diffusion (6).

The essential features of the model are these:

1. The reactor is divided into a hot zone or core where heat flow is assumed to be uniform over its cross section and given by Equation (1) at the inlet and thereafter by (2), and an isothermal cold zone or shell of constant cross section.

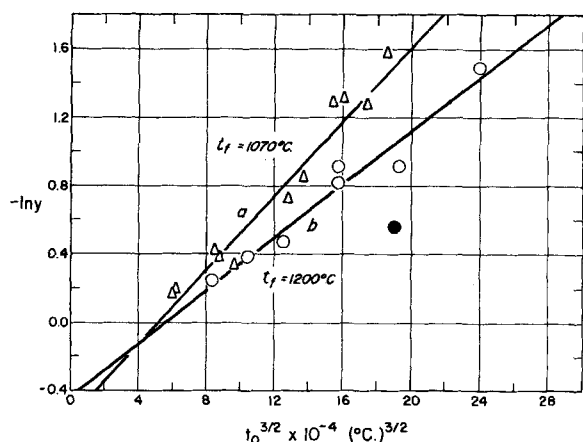


Fig. 3. $-\ln y$ vs. $t_o^{3/2}$ for ammonia: (a) 760 mm. Hg total pressure; intercept = -0.565 , and slope = 11.09×10^{-8} $(^\circ\text{C.})^{-3/2}$. (b) 300 mm. Hg total pressure; intercept = -0.440 , and slope = 7.8×10^{-8} $(^\circ\text{C.})^{-3/2}$. The filled point was disregarded when drawing the best straight line through the data.

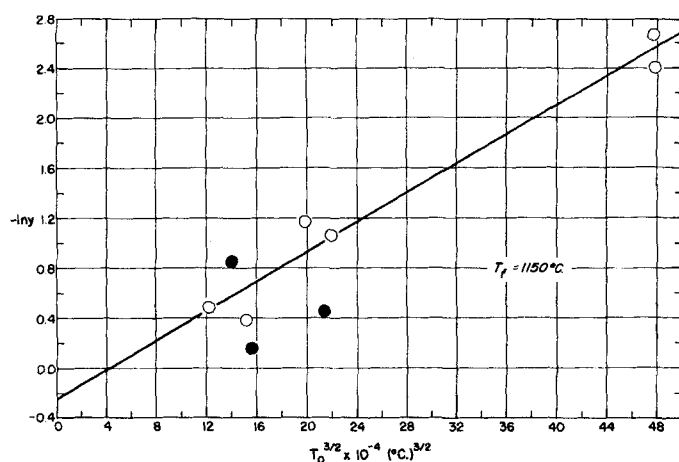


Fig. 4. $-\ln y$ vs. $t_o^{3/2}$ for methane at 300 mm. Hg total pressure. Intercept = -0.246 , slope = 5.87×10^{-8} $(^\circ\text{C.})^{-3/2}$. Open circles have less than 5% analytical error and were the only ones used in drawing the best line through data. Filled circles have more than 5% but less than 10% analytical error.

2. The pressure is taken to be uniform throughout the reactor. Note that this implies the molar flow rate of gas in the cold zone is everywhere a constant.

3. The reagent is assumed to be angularly plug fed into the cold zone of the reactor at a point $z = \sigma$. In the process an equal number of moles per unit time of argon are displaced from the cold zone into the hot zone.

4. The end of the reaction zone is defined as that point $z = b$, at which the mixed mean temperature of argon plus reagent falls below t_f ($^\circ\text{C.}$), some freezing temperature for the reaction.

5. The reaction is assumed infinitely fast for any reagent diffusing into the hot zone until the end of the reaction zone is reached. Beyond that point no reaction occurs.

6. The flow rate of reagent left in the cold zone as it crosses the point $z = b$ divided by the initial flow rate of reagent is just y .

7. No appreciable amount of the decomposition products builds up in the cold zone to restrict the postulated diffusion process to the radial counter-current diffusion of reagent out of, and argon into, the cold zone. Longitudinal diffusion is neglected.

This model is proposed as a reasonable first compromise between tractability and a rigorous physical description of the experiment. Assumption 3 is particularly doubtful because it is essentially the antithesis of the instantaneous mixing proposed for the dissociation-kinetics model, while the truth is almost certain to lie somewhere in between. One may nevertheless anticipate that if diffusion is indeed the controlling step, the actual geometry will be sufficiently noncritical to permit this degree of approximation.

Assumption 7 simply results (7) in Fick's second law of diffusion. Although

this vector differential equation should properly be solved in cylindrical coordinates for this problem to be consistent with assumption 3, it is considerably easier to solve it approximately as one dimensional diffusion out of a slab. (In any case because only the diffusion process in the cold zone is important, if this zone is very thin relative to the reactor diameter the two diffusion geometries become indistinguishable.) If x is the distance from the wall, Fick's differential equation may in this approximation be written as

$$\frac{\partial C}{\partial \tau} = D_{AB} \frac{\partial^2 C}{\partial x^2} \quad (4)$$

This differential equation may be solved for a cross section of the cold zone if one takes as boundary conditions no mass flow through the walls of the reactor and makes use of assumption 5, $C = 0$ at $x = \delta$.

The analogous but more general heat flux problem is solved elsewhere (8), so one may directly write down the solution

$$C = \frac{4 C_o}{\pi} \sum_{n=0}^{\infty} \frac{1}{2n+1} \exp \left\{ -\frac{D_{AB} (2n+1)^2 \pi^2 \tau}{4 \delta^2} \right\} \cos \left\{ \frac{(2n+1) \pi x}{2 \delta} \right\} \quad (5)$$

The number of reagent molecules entering at $z = \sigma$ per unit length of cold zone is just $\pi \delta C_o$. Integrating Equation (5) over the cross-section area of the cold zone gives the number of reagent molecules per unit length left at any time τ . The ratio of the second of these quantities to the first is just the fraction of reagent molecules left unconverted at time τ , y_τ :

$$y_\tau = \frac{8}{\pi^2} \sum_{n=0}^{\infty} \frac{1}{(2n+1)^2}$$

$$\exp \left\{ -\frac{D_{AB} (2n+1)^2 \pi^2 \tau}{4 \delta^2} \right\} \quad (6)$$

But the time τ is an easily determined function of distance from the point of mixing ($z - \sigma$):

$$\tau = \frac{z - \sigma}{u_c} = \frac{\pi (z - \sigma) p d \delta}{[\dot{m}/M]_c R T_c} \quad (7)$$

[Use has been made of the equation of continuity and the ideal gas law in deriving Equation (7).] One may therefore write

$$y_z = \frac{8}{\pi^2} \sum_{n=0}^{\infty} \frac{1}{(2n+1)^2} \exp \{ -K_n (z - \sigma) \} \quad (8)$$

where

$$K_n = \frac{\pi^3 (2n+1)^2 [D_{AB}]_c p d}{4 \delta [\dot{m}/M]_c R T_c} \quad (9)$$

In particular then, when $z = b$ and $t = t_f$, b is related to t_o through Equation (3):

$$b - \sigma = s(t_o/t_f)^{3/2} - (s + \sigma) \quad (10)$$

Substituting from (10) back into (8) one obtains

$$y = y_o = \frac{8}{\pi^2} \sum_{n=0}^{\infty} \frac{1}{(2n+1)^2} \exp \{ K_n (s + \sigma) \} \exp \left\{ -\frac{K_n s t_o^{3/2}}{t_f^{3/2}} \right\} \quad (11)$$

Except for the trivial case when $b = \sigma$ and its near vicinity, it is necessary to retain only the $n = 0$ term in the sum. Taking natural logarithms of the resulting expression one gets

$$\ln y + 0.209 = K(s + \sigma) - \frac{K s t_o^{3/2}}{t_f^{3/2}} \quad (12)$$

where

$$K = \frac{\pi^3 p d [D_{AB}]_c}{4 \delta [\dot{m}/M]_c R T_c} \quad (13)$$

Note that s is fixed by the geometry of the reactor through the enthalpy

profile expression, whereas σ is fixed by mixing geometry. By coincidence for this reactor $\sigma = s = 1.43$ cm. $[D_{AB}]_c$ is inversely proportional to pressure so K turns out to have no explicit pressure dependence. Furthermore $[D_{AB}]_c$ turns out to depend on T_c to the three-halves power so K depends on this parameter to the one-half power. Because of this weak dependence any reasonable value of this temperature may be used to test the model.

Results. Figure 3 is a plot of $\ln y$ vs. $t_c^{3/2}$ for ammonia at 760 mm. Hg total pressure and at 300 mm. Hg total pressure, while Figure 4 is the same plot for methane at 300 mm. Hg total pressure. Values of t_r obtained from slope and intercept of the best lines through the data are given in each case on the graph. These would appear to be reasonable values. Although the value for methane should only be regarded as crude, it is interesting that it should fall between the two values for ammonia, both rather carefully done. The substantial agreement between the values for ammonia at the two pressures is taken as partial verification of the model.

For the ammonia data at 760 mm. Hg total pressure, K as obtained from the intercept is just 0.27. It is interesting to insert reasonable values of the parameters in Equation (13) to evaluate δ . Penner (9) gives a procedure for calculating D_{AB} for several nonpolar gas systems. For $T_c = 600^\circ\text{K}$. and $p = 1$ atm. methane diffuses in argon with a D_{AB} of about 0.80. Presumably ammonia will not be much different. When one puts this in Equation (13), using $[m/M]_c$ of 0.00535 mole/sec. (corresponding to a typical ammonia flow rate) and a d of 0.635 cm., δ is just 0.055 cm. less than 10% of the reactor diameter. This is not at all an unreasonable value for this dimension.

At the present stage of plasma jet technology there would appear to be

no valid independent method to directly measure δ , but the value determined here is consistent with that inferred from the aforementioned heat transfer study (≈ 0.03 cm.). For ammonia at 300 mm. Hg total pressure, $K = 0.23$. As K has no explicit pressure dependence, this represents a 15% increase in δ which is still quite a reasonable value. Finally K for methane at 300 mm. Hg is 0.16, likely reflecting the relative crudeness of the methane data mainly but possibly indicating some difference in binary diffusion coefficient and thermal conductivity.

A final check on the consistency of the model is to calculate the required velocity in the boundary layer to see if it gives a reasonable value. An expression of u_c has already been used in obtaining δ . For ammonia at 760 mm. Hg total pressure the value is 2,500 cm./sec., which is 10% of the aerodynamically computed velocity. Although high for a boundary-layer velocity it is still sufficiently low to be credible. This value must therefore also be taken as consistent.

DISCUSSION

The good functional dependence of observed reaction yield on input power, reagent flow rate, and effluent plasma flow rate is not in itself sufficient corroboration of the diffusion-rate limited kinetics model. However the fact that very reasonable and consistent values of the adjustable parameter t_r were obtained in each case is a powerful confirmation of the general features of the model except perhaps for the exact mechanism of mixing. That δ also emerges with a reasonable value indicates that either a remarkable cancellation of errors occurs or else diffusion is indeed the important mixing mechanism and it was therefore correct to anticipate that the actual geometry would be relatively noncritical.

When one takes this latter point of view, it is of considerable interest to explore this model a little further to see what may be tentatively inferred about the nature of an intermediate section reactor. In this discussion the calculations are based on this reactor cracking ammonia at 760 mm. Hg with an argon flow rate of 0.016 g. moles/sec., an ammonia flow rate of 0.005 moles/sec., and a heat flow at the entrance to the reactor of 2,500 w. Equation (8) is assumed valid, while the adjustable parameters have been evaluated from the plot of Figure 3. The equations (parametric on z) representing the figures are rather lengthy but straightforward in derivation and are listed in the appendix.* The only ad-

ditional assumptions required in their derivation are:

1. Practically all of the effluent are plasma flows in the hot core.

2. As reagents diffuse into the hot zone and react the products are uniformly dispersed. This process is taken to be instantaneous so the convenient concepts of hot zone temperature and heat capacity are meaningful functions of axial position.

Product residence time

Figure 5 is a residence time distribution curve for cracking products in the reactor. The residence time is here rather arbitrarily defined as the interval between the time a molecule diffuses into the hot zone and the time its decomposition products cross t_r . In the figure $f d\tau$ is the fraction of those reagent molecules that will diffuse into the hot zone before t_r is crossed that spends between times τ and $\tau + d\tau$ in the hot zone or core of the reactor. Also included on the graph are values of the mean and median residence times. That the median and the mean both fall so close to the maximum value supports the aforementioned observation that mixing is very fast, since one half of the molecules have diffused into the hot zone in 60 $\mu\text{sec.}$ or within 1 cm. from the inlet for the reagent.

Temperature profile

Figure 6 is an initial temperature distribution which shows what fraction of the molecules that will ultimately diffuse into the hot zone before the end of the reactor will diffuse into mixed mean hot zone temperatures in excess of a temperature t . The nearly linear nature of this plot clearly poses a difficult problem for the systematic investigator.

Rate of quenching

One surprising aspect of the model is the abruptness with which the re-

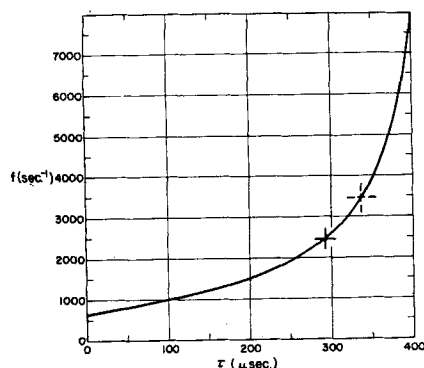


Fig. 5. Distribution of residence times for cracked reagent molecules in the hot zone of the reactor (see text for run description). The solid cross shows the mean residence time; the dashed cross, the median.

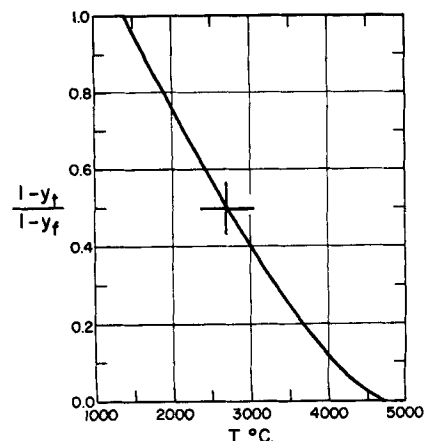


Fig. 6. The fraction of molecules eventually reacting that first see mixed mean hot zone temperatures in excess of any temperature t plotted vs. t . The cross marks the median temperature. Run conditions described in text.

* See footnote on page 451.

agent molecules cool the effluent plasma stream. Figure 7 is a plot of calculated hot core temperature vs. time with and without the reagent flow. Although the rate of temperature fall at the reactor entrance is high, the trend is impressively augmented by the addition of ammonia. The slope of the curve indicates a temperature decay rate of 5×10^7 deg./sec. when the ammonia first starts to mix. This may be stretching the crude model altogether too far, but the indicated use of a reactor of this type as a quenching device is clearly there.

CONCLUSION

The cracking behavior of ammonia and methane in a tube confined plasma jet has been shown rather conclusively to be rate limited by a diffusion process, and, in fact, a very good fit has been obtained to a particular model for the process. Although nothing can be learned about the actual dissociation kinetics, the characteristics of this type of reactor have been considerably clarified. For example for a particular gas mixture and power input the following quantities have been calculated:

1. The distribution of times spent by the products of decomposition in the reactor, the mean and the median.
2. The temperatures reagent molecules first encounter on diffusing into the hot zone.
3. The temperature vs. time profile of the effluent argon with reference to the possible use of this reactor as a quenching device.

ACKNOWLEDGMENT

The authors have conferred with many people in the course of this study and must acknowledge help from many sources. First of all, they are indebted to the technical assistance of Mr. C. W. Beville in the performance of the experiments. For helpful discussions relevant to the interpretation of the experiments, they wish to acknowledge Drs. Daniel Hyman, H. M. Hulburt, J. E. Longfield, Leon Lazare, R. L. Potter, and especially R. M. Griffith, all of this organization; Professors Michel Boudart of Princeton University, Paul Von Gross of Duke University, and Peter Harriott of Cornell University; as well as Mr. B. W. Wojciechowski of the University of Toronto. For freely discussing their relevant experimental work (in some cases still unpublished) the authors are indebted to Drs. G. B. Skinner and M. E. Gibbs of Monsanto Chemical Company; Carl Heath of Esso Research; T. A. Jacobs of the Jet Propulsion Center, California Institute of Technology; and Professor J. N. Holsen of Washington University.

NOTATION

- b = reactor length (determined by input enthalpy)
 C = local concentration of reagent gas (g. moles/cc.)

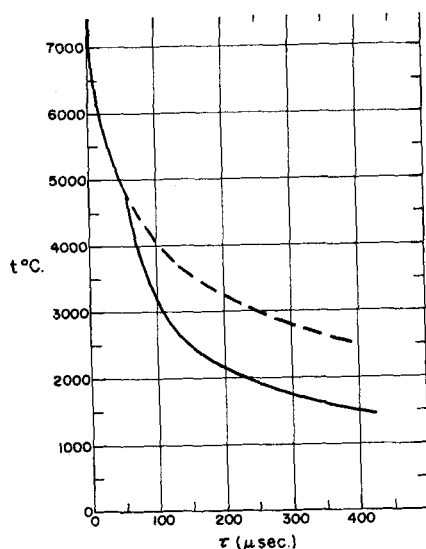


Fig. 7. Temperature vs. time for the argon effluent. Dashed line shows profile without reagent added, solid line shows profile with reagent. (Run conditions described in text.)

- c = heat capacity of cooling water (cal./g. °K.)
 d = reactor diameter (cm.)
 D_{AB} = binary diffusion coefficient for reagent gas in effluent plasma gas (sq. cm./sec.)
 E = arc voltage (v.)
 F = flow rate of cooling water (g./sec.)
 f = residence time distribution function (sec.⁻¹)
 h = $H^\circ - H^\circ_{298}$, the gas enthalpy in excess of ambient (cal./mole)
 I = arc current (amp.)
 K_n = lumped function defined in the text (cm.⁻¹)
 K = K_n , $n = 0$
 \dot{m}/M = molar flow rate of gas (g. moles/sec.)
 n_A = flow rate of argon (g. moles/sec.)
 n_G = flow rate of reagent gas (g. moles/sec.)
 p = pressure, taken as constant throughout the reactor (mm. Hg)
 q = net axial heat flow (at a particular axial position) averaged over the cross section (w.)
 R = universal gas constant (cc. mm. Hg/mole °K.)
 s = thickness of front electrode for this configuration (cm.)
 T = temperature (°K.)
 t = temperature (°C.)
 t_o = hypothetical temperature computed on the basis of fully mixed argon and reagent flows with the heat flow entering the intermediate section (°C.)
 t_f = freezing temperature (the mixed mean temperature below which molecules of re-

agent will not react on diffusing into the hot zone) (°C.)

- u = velocity (cm./sec.)
 x = linear dimension (distance from wall) in the equivalent problem of diffusion from a one dimensional slab (cm.)
 y = fraction of reagent introduced to the reactor remaining unconverted at any point. Without subscript this refers to the fraction remaining unconverted in the off gas.
 z = distance from the entrance of the intermediate section (cm.)
 δ = thickness of the cold zone or boundary layer (cm.)
 σ = value of z at point of reagent entry (cm.)
 τ = time (sec.)

Subscripts

- c = conditions in the cold zone
 i = i th water cooled section of plasma train
 n = running index on summation
 o = conditions at the entrance of the reactor ($z = 0$)
 z = conditions at axial position z
 σ = conditions at reagent inlet ($z = \sigma$)
 τ = condition of some molar envelope of gas at time τ after it enters the reactor

LITERATURE CITED

1. "JANAF Thermochemical Tables," Dow Chemical Company, Midland, Michigan (December 31, 1960).
2. Hougen, O. A., and K. M. Watson, "Chemical Process Principles," Vol. 3, Chap. 18, p. 832, Wiley, New York (1949).
3. Fowler, R., and E. A. Guggenheim, "Statistical Thermodynamics," Chap. 12, p. 521, Equation 1212.8, University Press, Cambridge, England (1952).
4. Matthews, J. C., M. E. Gibbs, and J. N. Holsen, paper presented at the 139 National meeting of the Am. Chem. Soc., St. Louis, Missouri (March 24, 1961).
5. Skinner, G. B., and R. A. Ruehrwein, *J. Phys. Chem.*, **63**, 1736 (1959).
6. Frank-Kamenetskii, D. A., "Diffusion and Heat Exchange in Chemical Kinetics," Chap. 2, Princeton University Press, Princeton, New Jersey (1955).
7. Bird, R. Byron, "Advances in Chemical Engineering," Vol. 1, p. 175, Academic Press, New York (1956).
8. Carslaw, H. S., and J. C. Jaeger, "Conduction in Heat in Solids," 2 ed., Chap. 3, p. 101, Equation 5, Oxford at the Clarendon Press, England (1959).
9. Penner, S. S., "Introduction to the Study of Chemical Reactions in Flow Systems," Chap. 2, p. 38, Butterworths Scientific Publications, London, England (1955).

Manuscript received September 1, 1961; revision received December 20, 1961; paper accepted December 22, 1961. Paper presented at A.I.Ch.E. New York Meeting.